Analysis of biomass and sewage sludge devolatilization using the distributed activation energy model

A. Soria-Verdugo *, N. Garcia-Hernando, L.M. Garcia-Gutierrez, U. Ruiz-Rivas

Carlos III University of Madrid (Spain), Energy Systems Engineering Group, Thermal and Fluids Engineering Department, Avda. de la Universidad 30, 28911 Leganés, Madrid, Spain

Abstract: The thermal decomposition of biomass (pine pellets) and sewage sludge was studied using thermogravi metric analysis under an inert atmosphere and the Distributed Activation Energy Model (DAEM) was employed. The activation energy and the frequency factor that characterize the kinetics were determined for both samples. A simplification of the process for prediction of devolatilization curves was proposed, evaluating its validity for both cases. The simplified method was found to combine both simplicity and low deviations with experimental data.

Keywords: DAEM, Biomass devolatilization, Pyrolysis kinetics, Sewage sludge.

1. Introduction

Biomass is gaining importance among the world final energy consumption because of its merits of being a renewable energy, widely distributed and carbon neutral [1]. Biomass is also a versa tile energy source, which can be used for power generation [2] and to produce liquid biofuels [3,4], synthesis gas [5], chemicals [6], or charcoal [7,8], via thermochemical processes such as combustion, gasification and liquefaction. Biomass pyrolysis takes place during these thermochemical processes. To establish the kinetics of pyro lysis many models have been developed, such as the single step model [9], the two parallel reaction model [10], the three pseu do component model [11], and the Distributed Activation Energy Model (DAEM).

The DAEM model was originally established by Vand [12] and it has been applied to a wide variety of complex reactions [13,14]. Miura [15] and Miura and Maki [16] developed a simple method to estimate the distributed activation energy and the corresponding frequency factor based on three TGA curves for different heating rates. They used their method to describe the pyrolysis of several kinds of coal. In the last years, this procedure has been thoroughly employed to analyze the kinetics of pyrolysis of different samples of coal [17,18], charcoal [19], oil shale [20], polymers [21], medical waste [22], and biomass [23 26].

The procedure established by Miura and Maki [16] to obtain the activation energy and the frequency factor is as follows: (i) measure the devolatilization rate for three different heating rates (a, usually between 3 and 30 K/min); (ii) calculate and plot $\ln(a/T^2)$ vs. $1/T$ at selected rates of devolatilization; (iii) determine the activation en ergy, E_a, and the frequency factor, k_0, from the slope and intercept in the Arrhenius plots at each rate of devolatilization; (iv) plot and dif ferentiate the values of E_a vs. the rate of devolatilization to obtain $f(E_a)$; and (v) predict other devolatilization rate curves for different heating rates.

In this study, a simplification is proposed to facilitate the recu peration or prediction of devolatilization curves. Thermogravimet ric tests were run to pyrolyse biomass and sewage sludge samples at three different heating rates under an inert atmosphere. The Miura and Maki [16] procedure and the proposed simplification were applied to both samples, obtaining their kinetics and quanti fying the differences between the experimental data and the dev olatilization curves obtained with the standard procedure and the proposed simplification.

2. Experimental

The proximate and ultimate analysis of the biomass (pine) and the sewage sludge samples are shown in Table 1, together with the heating values. The proximate analysis was carried out in a TGA Q500 TA Instruments while the ultimate analysis was run in a LECO TruSpec CHN and TruSpec S analyzer. The heating value of the samples was determined in a Parr 6300 calorimeter.

The results of the proximate and the ultimate analyses of the pine samples are comparable to those of Biagini et al. [27], Shen et al. [26], and Navarro et al. [28]. On the other hand, the results for the sewage sludge can be compared to those of Scott et al.

* Corresponding author. Tel.: +34 916248884; fax: +34 916249430.
E-mail address: asoria@ing.uc3m.es (A. Soria-Verdugo).

Nomenclature

a	heating rate [K/s]	T	temperature [K]
E_a	activation energy for a determine devolatilization rate [J/mol]	V	volatile mass loss [%]
		V^*	volatile content [%]
k_0	pre exponential factor for a determine devolatilization rate [s^{-1}]	V/V^*	devolatilization rate [%]
R	universal constant [J/mol K]		

[29], although in this case there are higher differences due to the great heterogeneity of sewage sludge.

Thermogravimetric analysis was carried out at three different heating rates (10, 15 and 20 K/min) with dry samples. A flow rate of 60 ml/min of nitrogen was supplied to the furnace in order to maintain the samples in an inert atmosphere. A mass of 10±0.5 mg of the samples, previously sieved under 100 μm, was employed to avoid the effect of heat and mass transfer during the thermal decomposition [30]. Each test was repeated five times obtaining differences lower than 3% to guarantee repeatability. A blank experiment was also run to exclude a buoyancy effect [26].

3. Results

Fig. 1 shows the devolatilization curves of biomass (a) and sew age sludge (b) for the three different heating rates. The devolatiliza tion of biomass occurred at a lower temperature, between 100 and 600 °C, while operating with sewage sludge, the temperature must be as high as 1000 °C to reach a high conversion rate [29]. The tem peratures at which pine conversion occurs are in good agreement to those obtained by Biagini et al. [27] and Navarro et al. [28], and they are also similar to those obtained by Sonobe et al. [25] who analyzed the devolatilization of biomasses with a high content of cellulose.

The biomass employed reached a high conversion in a reduced range of temperature, a typical result for samples with a high content of cellulose [25]. On the other hand, the devolatilization process of sewage sludge occurred in a wide range of tempera tures. These two samples were considered to be a limit concerning the velocity of the devolatilization processes, from the quick devol atilization for the pine sample to the slow devolatilization of the sewage sludge.

From the data in Fig. 1, a $\ln(a/T^2)$ vs. $1/T$ plot for each heating rate, a, at selected values of the devolatilization rate was built and presented in Fig. 2.

The activation energy, E_a, and the frequency factor, k_0, can now be obtained from the slope and intercept in the Arrhenius plots at each rate of devolatilization. Each curve is represented by Eq. (1), as stated by Miura and Maki [16] (being their Eq. (10)). It immedi ately follows that, for the curves shown in Fig 2, of the form (m 1/ $T + n$), E_a and k_0 can be obtained with Eqs. (2) and (3) respectively.

$$\ln\left(\frac{a}{T^2}\right) \quad \ln\left(\frac{k_0 R}{E_a}\right) + 0.6075 \quad \frac{E_a}{R}\frac{1}{T} \tag{1}$$

$$E_a \quad m \cdot R \tag{2}$$

$$k_0 \quad m \cdot \exp(n \quad 0.6075) \tag{3}$$

where T is the temperature and R the universal constant.

Fig. 3 shows the activation energy (graph a) and the frequency factor (graph b) obtained for the biomass and sewage sludge sam ples. The values of the activation energy and the frequency factor for the biomass, between 160 and 270 kJ/mol, and between 10^{11} and 10^{16} s^{-1} respectively, are in accordance with the values ob tained in the literature for pine samples [26 28] and for similar biomasses such as cotton straw [23], rice husk [25], and barley [31]. In the case of the sewage sludge sample a higher activation energy was obtained, between 170 and 400 kJ/mol corresponding also to higher values of the frequency factor, which ranges between 10^{12} and 10^{20} s^{-1} and sometimes even higher. Although the very large values may not represent the actual physics due to the error inherent to the method, the results are in accordance with others found in the literature [29].

4. Prediction of devolatilization curves: a simplification of the standard procedure

There are several ways to predict other devolatilization curves once the activation energy and the frequency factor are known for each devolatilization rate. First, one can obtain $f(E_a)$ from the data of Fig. 3a, and directly apply the DAEM model to calculate the rate of devolatilization, V/V^* for a given heating curve, using the fowolling erquation:

$$1 \quad \frac{V}{V^*} \quad \int_0^\infty \exp\left(\quad k_0 \int_0^t e^{\ E_a/(RT)} dt \right) \cdot f(E_a) \cdot dE_a \tag{4}$$

where V is the volatile mass loss, V^* is the volatile content, and V/V^* is the devolatilization rate.

A simpler procedure, when the data of Fig. 2 is available, permits to determine the temperature at which devolatilization occurs for a given heating rate by solving the transcendental equa tion presented as Eq. (1). Then, the procedure from Figs. 1 and 2 should be performed inversely.

This procedure could be further simplified. Fig. 2 shows that the data points obtained for each particular heating rate could be lin earized. In Fig. 4a, the $\ln(1/T^2)$ vs. $1/T$ plot for all the data points are presented, together with the linearization. Note that a is now missing and all the curves collapse. Of course, the data points fol low a quadratic curve in this plot, but for the usual range of tem perature (200 800 °C) the error between the linearization and the quadratic curve is small, as shown in Fig. 4b.

Table 1
Properties of the samples.

	Biomass (pine)	Sewage sludge
Proximate analysis[a]		
Moisture (%)	3.85	5.98
Volatiles (%)	78.08	58.97
Fixed carbon[b] (%)	14.69	9.41
Ash (%)	3.38	25.64
Ultimate analysis[c]		
C (%)	49.72	45.39
H (%)	7.02	7.69
N (%)	0.88	6.95
S (%)	0.07	1.78
O[b] (%)	42.31	38.19
High heating value[a] (MJ/kg)	18.46	11.58

[a] Wet basis.
[b] Obtained by difference.
[c] Dry-ash-free basis.

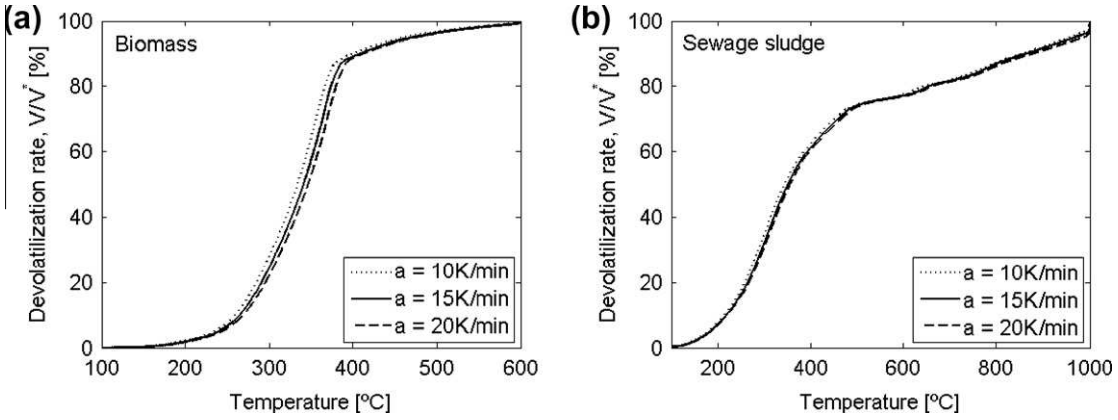

Fig. 1. Devolatilization rate of the biomass sample (a) and the sewage sludge sample (b).

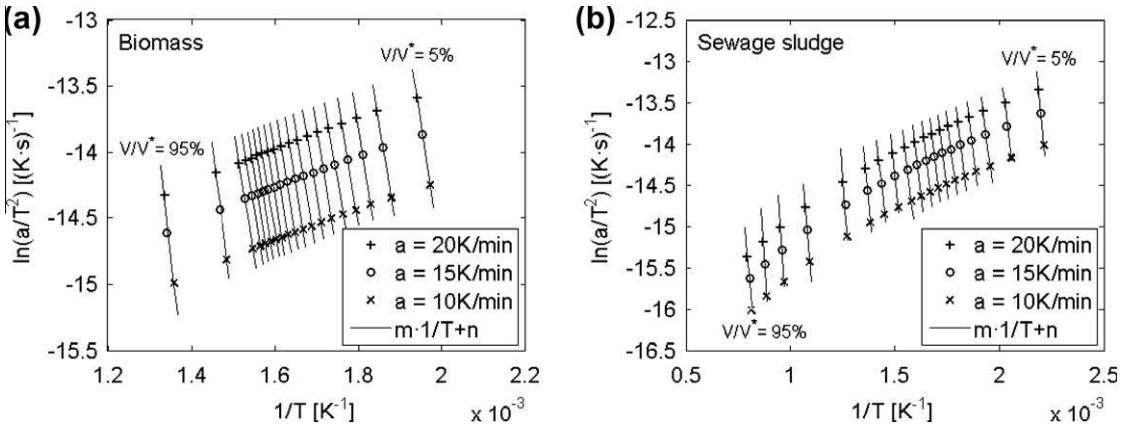

Fig. 2. $\ln(a/T^2)$ vs. $1/T$ for devolatilization rates variations of 5%, for the biomass sample (a) and the sewage sludge sample (b).

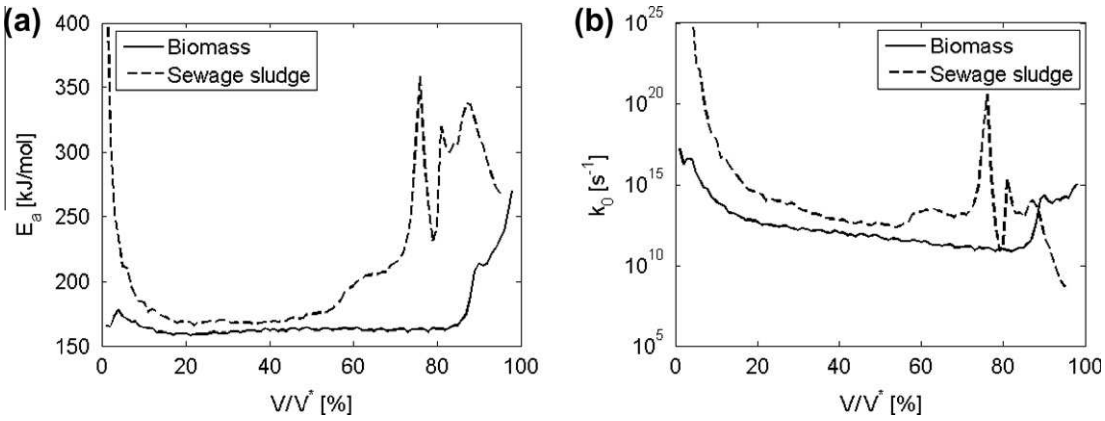

Fig. 3. Activation energy (a) and frequency factor (b).

Using the linearization for each heating rate, the temperature at which devolatilization occurs can be determined in the intersec tion between the linearization for a heating rate and the lineariza tion for each devolatilization rate, as shown in Fig. 5 for the biomass sample.

Therefore, the temperature for a determined devolatilization rate can be calculated as the intersection between the two equa tions shown in Fig. 5. This results in the following equation:

$$T \quad \frac{E_a/R \quad 1194}{\ln(a) \quad 15.40 \quad \ln(\frac{k_0 R}{E_a})} \tag{5}$$

where T is the temperature for a determined devolatilization rate, a is the heating rate, E_a is the activation energy, k_0 is the frequency factor, and R is the universal constant.

The direct prediction of the temperature at which a determined devolatilization rate occurs using Eq. (5) is easier than the process employed with the existing DAEM models.

The error of the procedure was characterized. The devolatiliza tion curves were recuperated using the standard procedure solv ing Eq. (1) and using the simplification employing Eq. (5) for the biomass and sewage sludge samples. In Fig. 6, the experimental devolatilization curves are plotted together with the curves recu

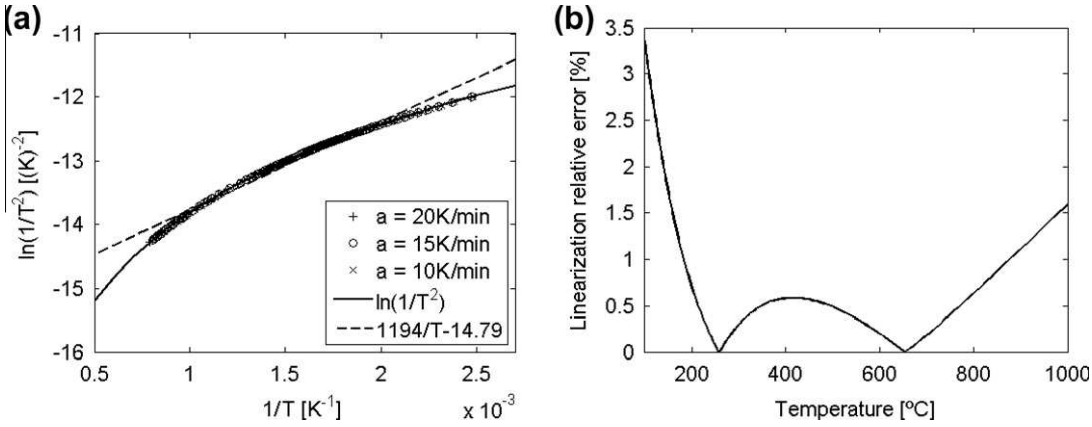

Fig. 4. (a) Linearization of the $\ln(a/T^2)$ vs. $1/T$ curves for varying devolatilization rate and (b) linearization relative error.

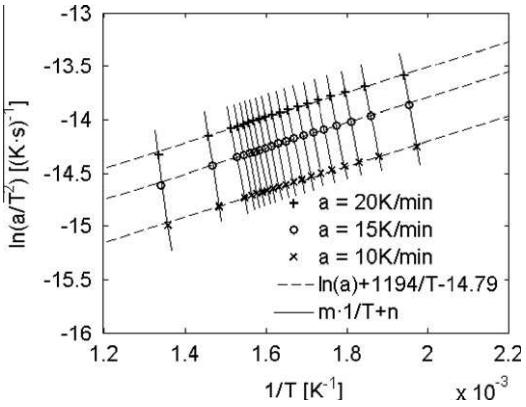

Fig. 5. Determination of the temperature at which devolatilization of biomass occurs.

perated with the simplification. In this figure, only the curve corre sponding to a heating rate of 20 K/min is plotted for the two sam ples. The results for the 10 15 K/min are very similar.

Fig. 6 does not show any mismatch. The differences in tempera ture for each devolatilization rate were analyzed to state the actual discrepancies. Fig. 7 shows the differences in temperature between the experimental data and the curves obtained with Eq. (5). The er ror plotted in Fig. 7 is found to be larger for the sewage sludge sam ple due to the higher temperature needed for the devolatilization in this case. Concerning the error obtained for the biomass, a higher value is obtained for the lowest and highest devolatilization rates. The error obtained for each heating rate is quite similar for the two samples. Considering the temperature at which each devolatil ization occurs, the maximum relative error between the experi mental temperature and that obtained by the simplified DAEM model is less than 0.35% for the biomass and less than 1.2% for the sewage sludge sample. Therefore, the recuperation is found to be accurate.

The error committed when recuperating the devolatilization curves following and existing DAEM method, that is solving Eq. (1), is also plotted in Fig. 8. Thus, comparing Figs. 7 and 8 the validity of the simplified DAEM model might be analyzed. The error obtained for the biomass sample is quite similar for both the simplified and the existing DAEM model, nonetheless the sim plified model reduces slightly the error for high devolatilization rates. A similar tendency is found for the sewage sludge sample, obtaining minor differences for low and medium devolatilization rates and a slight improvement in the recuperation of the devola tilization curves of 10 20 K/min when applying the simplified DAEM model. The existing DAEM model reached slightly lower er rors just for the case of the sewage sludge curve obtained at a heat ing rate of 15 K/min. The errors for both the simplified and the existing DAEM model were in all the cases reduced, obtaining a good match between the experimental devolatilization curves and the curves recuperated for the models, as shown in Fig. 6. Therefore, the simplification described by Eq. (5) can be said to be an useful tool for the prediction of devolatilization curves.

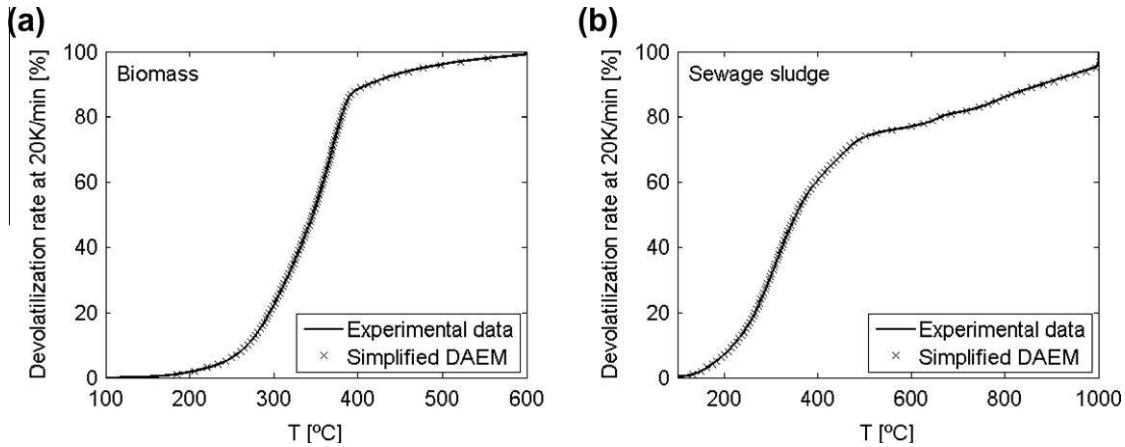

Fig. 6. Recuperation of the devolatilization curves using Eq. (5) for (a) biomass and (b) sewage sludge.

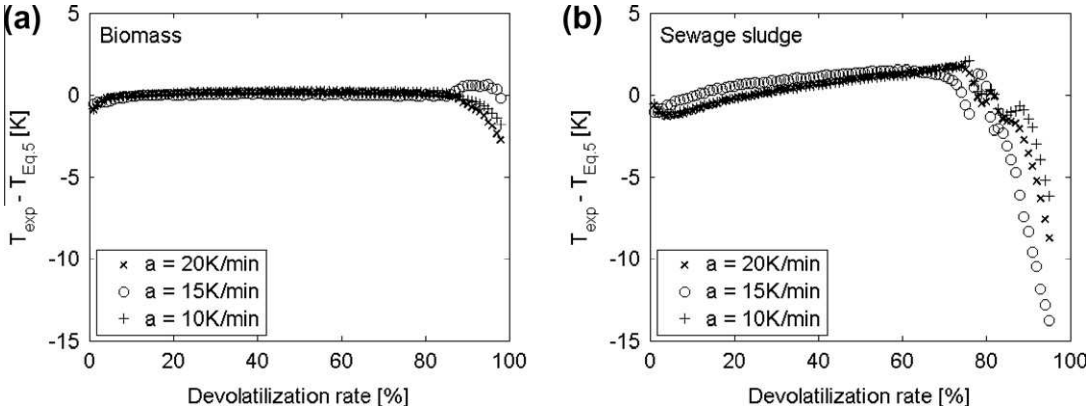

Fig. 7. Temperature difference between the experimental data and the data obtained using Eq. (5) for (a) the biomass and (b) the sewage sludge samples.

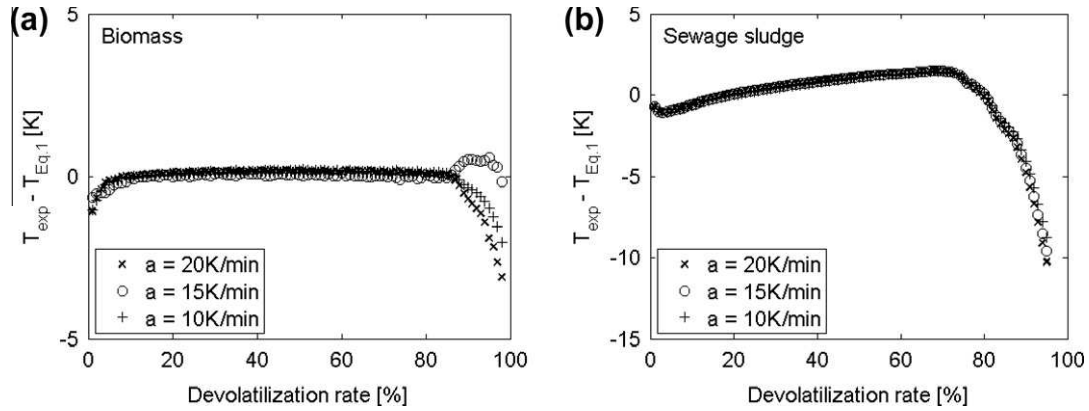

Fig. 8. Temperature difference between the experimental data and the DAEM model (Eq. (1)) for (a) the biomass and (b) the sewage sludge samples.

5. Conclusions

Thermogravimetric curves obtained under an inert atmosphere at three different heating rates (10, 15 and 20 K/min) were em ployed to analyze the devolatilization process of biomass and sew age sludge using DAEM. The activation energy obtained for the biomass sample (from pine pellets) is in the range of 160 270 kJ/ mol, and the frequency factor was in the range of 10^{11} 10^{16} s^{-1}, which is in accordance with the reported values in the literature. The sewage sludge sample showed higher activation energies, from 170 to 400 kJ/mol, and frequency factors ranging between 10^{12} and 10^{20} s^{-1} and even higher. These values are also in accordance with previous studies.

A simplification was suggested for predicting devolatilization curves for different heating rates. The differences between the temperature predicted by the simplified method and experimental data were quantified, obtaining relative errors smaller than 0.35% for the biomass and 1.2% for the sewage sludge sample. Compared with the standard procedure, the simplified DAEM model obtained a slight improvement for high devolatilization rates.

Acknowledgments

This work has been partially supported by the National Energy Program of the Spanish Department of Science and Education (ENE2006 01401), the Spanish Government (DPI2009 10518 MICINN) and the Madrid Community (CCG07 uc3 m/amb 3412, CCG08 uc3 m/amb 4227 and P2009/ENE 1660).

References

[1] Senneca O. Kinetics of pyrolysis, combustion and gasification of three biomass fuels. Fuel Process Technol 2007;88:87–97.
[2] Kazagic A, Smajevic I. Experimental investigation of ash behavior and emissions during combustion of Bosnian coal and biomass. Energy 2007;32:2006–16.
[3] Asadullah M, Anisur Rahman M, Mohsin Ali M, Abdul Motin M, Borhanus Sultan M, Robiul Alam M, et al. Jute stick pyrolysis for bio-oil production in fluidized bed reactor. Bioresour Technol 2007;99:44–50.
[4] Pütün AE, Burcu Uzun B, Apaydin E, Pütün E. Bio-oil from olive oil industry wastes: pyrolysis of olive residue under different conditions. Fuel Process Technol 2005;87:25–32.
[5] Kaewluan S, Pipatmanomai S. Potential of synthesis gas production from rubber wood chip gasification in a bubbling fluidised bed gasifier. Energy Conv Manage 2011;52:75–84.
[6] Orecchini F, Bocci E. Biomass to hydrogen for the realization of closed cycles of energy resources. Energy 2007;32:1006–11.
[7] Prauchner MJ, Pasa VMD, Molhallem NDS, Otani C, Otani S, Pardini LC. Structural evolution of Eucalyptus tar pitch-based carbons during carbonization. Biomass Bioenergy 2005;28:53–61.
[8] Prins MJ, Ptasinski KJ, Janssen FJJG. Torrefaction of wood. Part 1. Weight loss kinetics. J Anal Appl Pyrol 2006;77:28–34.
[9] Coats AW, Redfern JP. Kinetic parameters from thermogravimetric data. Nature 1964;201:68–9.
[10] Ubhayacar SK, Stickler DB, Von Rosenberg CW, Gannon RE. Rapid devolatilization of pulverized coal in hot combustion gases. In: 16th Symposium combust; 1976.
[11] Li Z, Zhao W, Meng B, Liu C, Zhu Q, Zhao G. Kinetic study of corn straw pyrolysis: comparison of two different three-pseudocomponent models. Bioresour Technol 2008;99:7616–22.
[12] Vand V. A theory of the irreversible electrical resistance changes of metallic films evaporated in vacuum. Proc Phys Soc 1942;A55:222–46.
[13] Pitt GJ. The kinetics of the evaluation of volatile products from coal. Fuel 1962;41:267–74.
[14] Lakshmanan CC, Bennet ML, White N. Implications of multiplicity in kinetic parameters to petroleum exploration distributed activation energy models. Energy Fuels 1991;5:110–7.

[15] Miura K. A new and simple method to estimate $f(E)$ and $k_0(E)$ in the distributed activation energy model from three sets of experimental data. Energy Fuels 1995;9(302):307.
[16] Miura K, Maki T. A simple method for estimating $f(E)$ and k0(E) in the distributed activation energy model. Energy Fuels 1998;12:864–9.
[17] Günes M, Günes SK. Distributed activation energy model parameters of some Turkish coals. Energy Sources. Part A. Recov Utiliz Environ Effects 2008;30:1460–72.
[18] Li Z, Liu C, Chen Z, Qian J, Zhao W, Zhu Q. Analysis of coals and biomass pyrolysis using the distributed activation energy model. Bioresour Technol 2009;100:948–52.
[19] Várghegyi G, Szabó P, Antal MJ. Kinetics of charcoal devolatilization. Energy Fuels 2002;16:724–31.
[20] Wang Q, Wang H, Sun B, Bai J, Guan X. Interactions between oil shale and its semi-coke during co-combustion. Fuel 2009;88:1520–9.
[21] Wanjun T, Cunxin W, Donghua C. Kinetic studies on the pyrolysis of chitin and chitosan. Polym Degrad Stab 2005;2005(87):389–94.
[22] Yan JH, Zhu HM, Jiang XG, Chi Y, Cen KF. Analysis of volatile species kinetics during typical medical waste materials pyrolysis using a distributed activation energy model. J Hazard Mater 2009;162(646):651.
[23] Hu S, Jess A, Xu M. Kinetic study of Chinese biomass slow pyrolysis: comparison of different kinetic models. Fuel 2007;86:2778–88.
[24] Cai J, Liu R. New distributed activation energy model: numerical solution and application to pyrolysis kinetics of some types of biomass. Bioresour Technol 2008;99:2795–9.
[25] Sonobe T, Worasuwannarak N. Kinetic analyses of biomass pyrolysis using the distributed activation energy model. Fuel 2008;87:414–21.
[26] Shen DK, Gu S, Jin B, Fang MX. Thermal degradation mechanisms of wood under inert and oxidative environments using DAEM methods. Bioresour Technol 2011;102:2047–52.
[27] Biagini E, Lippi F, Petarca L, Tognotti L. Devolatilization rate of biomasses and coal-biomass blends: and experimental investigation. Fuel 2002;81:1041–50.
[28] Navarro MV, Murillo R, Mastral AM, Puy N, Bartroli J. Application of the distributed activation energy model to biomass and biomass constituents devolatilization. AIChE Journal 2009;55:2700–15.
[29] Scott SA, Dennis JS, Davidson JF, Hayhurst AN. Thermogravimetric measurements of the kinetics of pyrolysis of dried sewage sludge. Fuel 2006;85:1248–53.
[30] Di Blasi C, Branca C, Santoro A, Gonzalez Hernandez E. Pyrolytic behavior and products of some wood varieties. Combust Flame 2001;124:165–77.
[31] Várhegyi G, Chen H, Godoy S. Thermal decomposition of wheat, oat, barley, and Brassica Carinata straws, a kinetic study. Energy Fuels 2009;23:646–52.